Pions and Strange Mesons in a Modified Soft-Wall Model of AdS/QCD

September 14, 2011

Sean P. Bartz
School of Physics and Astronomy
University of Minnesota
116 Church St. SE, Minneapolis, MN 55455, USA

1 Introduction

Quantum chromodynamics (QCD), the theory describing the strong nuclear force, has yet to be solved analytically, despite the extensive research of the past thirty-five years. Recently, the Anti-de Sitter space/conformal field theory correspondence (AdS/CFT) has brought hope of reformulating QCD into an analytically solvable theory. This gauge/gravity duality is a result from string theory that relates strongly-coupled gauge theories in D dimensions to weakly-coupled gravity in $D+1$ curved spacetime dimensions [1]. Calculations that are impossible in the non-perturbative gauge theory can be related to perturbative results from the gravity theory using the AdS/CFT dictionary [2, 3]. Although QCD has only approximate conformal symmetry in its high-energy limit, it has been conjectured that QCD may possess a suitable 5D gravity dual for such analysis [4, 5]. Such studies are known as AdS/QCD or holographic QCD. "Top-down" models start with a string theory and attempt to find a gravitational background that will reproduce basic QCD features. A more phenomenological approach is the "bottom-up" model, which begins with QCD observables and builds a 5D gravity model that reproduces these features [5].

Confinement breaks the conformal symmetry of QCD. This is incorporated in AdS/QCD by a mechanism that prevents the fields from penetrating deeply into the bulk. The simplest way to achieve this is through a hard cutoff related to the QCD

mass scale, as seen in the "hard-wall" model [5, 6]. This model fails to accurately model the spectrum of the radially excited meson states, predicting a quadratic trajectory $m_n^2 \sim n^2$, as opposed to the linear trajectory $m_n^2 \sim n$ expected [7]. A linear trajectory can be found by implementing a "soft-wall" model, where the 5D action is multiplied by a dilaton field ϕ, which decreases the action at large z [8]. The linear mass trajectory for the mesons is recovered when $\phi(z) \sim z^2$ at large z.

Chiral symmetry is broken explicitly by the quark mass and spontaneously by the presence of a quark condensate. The breaking of this symmetry is responsible for the non-zero mass of the pion and the mass splitting between the vector and axial-vector mesons. These types of chiral symmetry breaking occur independently in QCD, which must be reflected in an AdS/QCD model. In addition, the model must ensure that chiral symmetry is not restored for the highly excited states of the vector and axial mesons [9].

This paper uses a bottom-up soft-wall AdS/QCD model based upon [8] to model the mass spectra of the radial excitations of the mesons. Section 2 presents a modified simple soft-wall model from the work in [10], which obtains the correct form of chiral symmetry breaking while also improving the predicted mass spectra for the scalar, vector, and axial sectors. Section 3 describes the continuation of this model to accurately model the pseudoscalar sector [11]. Finally, Section 4 describes the ongoing work to expand this soft-wall model by including the strange quark.

2 Modified Soft-Wall Model

The four-dimensional fields of QCD live on a surface in the five-dimensional anti-de Sitter space, with a metric given by

$$ds^2 = a^2(z)(\eta_{\mu\nu}dx^\mu dx^\nu + dz^2), \qquad z \geq 0, \tag{1}$$

where $a(z) = L/z$ is the warp factor and L is the AdS curvature radius. The bulk coordinate z is associated with inverse energy scales, with the ultraviolet limit of QCD represented by fields at $z \to 0$ [4]. The AdS/CFT dictionary [1, 2] states that each operator $\mathcal{O}(x)$ in the 4D conformal field theory is associated with a bulk field $\psi(x, z)$. The values of the bulk fields at the UV boundary act as sources for the corresponding 4D currents. Global symmetries of the 4D field theory become gauged symmetries for the bulk fields.

The field content of the 5D theory is dictated by the operators relevant to the chiral dynamics of QCD. The gauge fields $A_{L\,\mu}$, $A_{R\,\mu}$ correspond to the left- and right-handed currents of the $SU(N_f)_L \times SU(N_f)_R$ chiral symmetry, where N_f is the number of quark flavors in the model. The scalar field X is associated with the chiral operator $\overline{q}q$ [5]. The masses of the bulk fields are set by the AdS/CFT relation [12] $m_5^2 L^2 = (\Delta - p)(\Delta + p - 4)$, where Δ is the dimension of the p-form QCD operator.

4D Operator	5D Field	p	Δ	$m_5^2 L^2$
$\overline{q_L}\gamma^\mu t^a q_L$	$A^a_{L\,\mu}$	1	3	0
$\overline{q_R}\gamma^\mu t^a q_R$	$A^a_{R\,\mu}$	1	3	0
$\overline{q}^\alpha_R q^\beta_L$	$\frac{2}{z}X^{\alpha\beta}$	0	3	-3

Table 1: Operators and fields of the model. The matrices t^a are the generators of the $SU(N_f)$ symmetry.

Table 1 illustrates the fields and operators of our model, showing that the scalar field is the only massive field in this model.

The simplest soft-wall action involving the fields from Table 1 is given in [8]. This action was modified in [10] with the addition of a quartic term in the scalar potential, yielding

$$S_5 = \int d^5x\sqrt{-g}e^{-\phi(z)}Tr\left[|DX|^2 + m_X^2|X|^2 - \kappa|X|^4 + \frac{1}{2g_5^2}(F_A^2 + F_V^2)\right], \qquad (2)$$

The $5D$ gauge coupling constant g_5 is fixed by calculating the vector current two-point function using this model and then comparing this to the leading order result from QCD, leading to the identification $g_5^2 = 12\pi^2/N_c$ [5]. The parameter κ is fit using the meson mass spectra. The field X includes both the scalar and pseudoscalar fields in a representation that will be discussed in Section 3.1. The field strength tensors and covariant derivative are defined as

$$F^{MN}_{L,R} = \partial^M A^N_{L,R} - \partial^N A^M_{L,R} - i[A^M_{L,R}, A^N_{L,R}]$$

$$D^M X = \partial^M X - iA^M_L X + iXA^M_R.$$

To describe the vector and axial-vector mesons, we define the fields $V^M = \frac{1}{2}(A^M_L + A^M_R)$ and $A^M = \frac{1}{2}(A^M_L - A^M_R)$. It is convenient to write the action in terms of the fields that describe physical particles with the following re-definitions

$$(F_A^2 + F_V^2) = 2(F_L^2 + F_R^2) \qquad (3)$$

$$D_M X = \partial_M X - i\{A^a_M, X\} + i[V^a_M, X] \qquad (4)$$

The scalar field X takes on a z-dependent vacuum expectation value (VEV), breaking the chiral symmetry. In a flavor-symmetric model, the VEV has the form $X_0 = \langle X\rangle = \frac{v(z)}{2}I$, where I is the $N_f \times N_f$ identity matrix. From the AdS/CFT dictionary established in [1, 2], $v(z)$ has the ultraviolet asymptotic form

$$\lim_{z\to 0} v(z) = m_q z + \sigma z^3, \tag{5}$$

where m_q is the quark mass and $\sigma = \langle \overline{q}q \rangle$ is the chiral condensate, the variation of the vacuum energy with respect to m_q.

Taking $X = X_0$ and varying (2), we find that $v(z)$ has the following nonlinear equation of motion:

$$\partial_z(a^3 e^{-\phi}\partial_z v(z)) - a^5 e^{-\phi}\left(m_X^2 v(z) - \frac{\kappa}{2}v^3(z)\right) = 0. \tag{6}$$

The UV asymptotic form is given by (5), while the non-restoration of chiral symmetry dictates that $v(z) \sim z$ in the infrared region. The VEV is parameterized so that it matches the expected asymptotic behavior. A suitable form was found and justified in [10]

$$v(z) = \alpha z + \beta \tanh(\gamma z^2) \tag{7}$$

with the parameters defined as follows

$$\alpha = \frac{\sqrt{3}m_q}{g_5 L}, \qquad \beta = \sqrt{\frac{4\lambda}{\kappa L^2}} - \alpha, \qquad \gamma = \frac{g_5\sigma}{\sqrt{3}\beta}.$$

The quark mass and chiral condensate can each be taken to zero independently, and the non-restoration of chiral symmetry does not depend on either of these parameters. Thus, the spontaneous and chiral symmetry breaking occur separately, as desired [10]. Using (7) in (6) we can solve for the dilaton field.

Equations of motion are then derived using a variational principle. The eigenvalues cannot be found analytically, so a numerical shooting method is used to calculate the mass spectra for the scalar, vector, and axial sectors. The results for the vector mesons are shown in Figure 1, and the scalar and axial sectors show similarly good results [10]. These results reproduce the linear trajectories found in the simple soft-wall model [8] for large n, while improving the agreement of the lower excitations with data.

3 Pions in Soft-Wall AdS/QCD

This modified soft-wall model was later completed in the paper [11], which clarified the discrepancies between two common representations of the pseudoscalar field, calculated the pion mass spectrum to good accuracy, and derived the Gell-Mann–Oakes–Renner relation from the model.

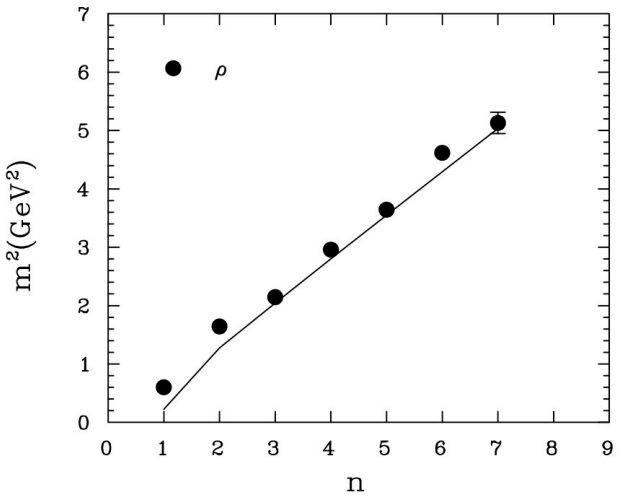

Figure 1: Radial excitations of the ρ meson [13] compared to numerical solution.

3.1 Pseudoscalar Representation

As mentioned above, the field X contains both the field representing the scalar mesons, S, and the field representing the pseudoscalars, π, as well as the VEV. There are two common ways to represent this field:

$$X_e = \left(\frac{v(z)}{2} + S(x,z)\right) I e^{2i\pi_e(x,z)^a t^a} \tag{8}$$

$$X_l = \left(\frac{v(z)}{2} + S(x,z)\right) I + i\pi_l(x,z)^a t^a \tag{9}$$

with I the $N_f \times N_f$ identity matrix and t^a the $SU(N_f)$ generators. We will refer to X_e as the exponential representation and X_l as the linear representation.

Let us take (8) and substitute it into (2), keeping terms that include the field $\pi(\mathbf{x}, z)$, as well as terms that will mix with π. We work in the axial gauge, $A_z = 0$, and separate A_μ into its transverse and longitudinal components: $A_\mu = A_{\mu\perp} + \partial_\mu\varphi$ where $\partial_\mu A^\mu_\perp = 0$. Separating explicitly into regular 4D components and extra-dimensional terms, and expressing it in terms of the longitudinal part of A_μ gives

$$\begin{aligned}\mathcal{L}_e &= -\frac{1}{2}\mathrm{e}^{-\phi(z)}\Big[\sqrt{-g}g^{\mu\nu}(v^2\partial_\mu\pi\partial_\nu\pi + v^2\partial_\mu\varphi\partial_\nu\varphi - 2v^2\partial_\mu\pi\partial_\nu\varphi) \\ &\quad + \sqrt{-g}g^{zz}v^2\partial_z\pi\partial_z\pi \; + \frac{\sqrt{-g}g^{zz}g^{\mu\nu}}{g_5^2}(\partial_z\partial_\mu\varphi\partial_z\partial_\nu\varphi)\Big].\end{aligned} \tag{10}$$

Varying (10) with respect to π and performing a Kaluza-Klein decomposition,expressing

the system of equations in terms of its z-dependent parts.

$$e^{\phi}\partial_z\left(\frac{e^{-\phi}v^2}{z^3}\partial_z\pi_n\right)+\frac{v^2m_n^2}{z^3}(\pi_n-\varphi_n)=0. \tag{11}$$

Varying (10) with respect to φ and breaking it down into KK modes gives the second equation of motion

$$\mathrm{e}^{\phi}\partial_z\left(\frac{\mathrm{e}^{-\phi}}{z}\partial_z\varphi_n\right)+\frac{g_5^2L^2v^2}{z^3}(\pi_n-\varphi_n)=0. \tag{12}$$

We then substitute the linear representation of the scalar field into the original Lagrangian. Following the same procedure as above, we derive two coupled equations. Varying with respect to φ produces

$$\mathrm{e}^{\phi}\partial_z\left(\frac{\mathrm{e}^{-\phi}}{z}\partial_z\varphi_n\right)+\frac{g_5^2L^2v}{z^3}\left(\pi_n-v\varphi_n\right)=0. \tag{13}$$

Varying with respect to π gives the second equation of the linear representation

$$z^3\mathrm{e}^{\phi}\partial_z\left(\frac{\mathrm{e}^{-\phi}}{z^3}\partial_z\pi_n\right)-\left(\frac{m_X^2}{z^2}-\frac{\kappa L^2v^2}{2z^2}\right)\pi_n+m_n^2\pi_n=m_n^2v\varphi_n. \tag{14}$$

3.2 Representation Equivalence

The pseudoscalar field representation should not affect the physical results obtained from the model. It is therefore desirable to show that the equations of motion derived from the two representations are equivalent.

We begin by expanding X_e to first order in the fields

$$\begin{aligned} X_e &= \left(\frac{v}{2}+S\right)(1+2i\pi_e+\ldots) \\ &= \frac{v}{2}+S+i\pi_e v. \end{aligned} \tag{15}$$

Comparing (15) to (9), we surmise that $\pi_e v(z)\rightarrow\pi_l$ is the relationship between the two representations. Let us substitute $\pi_e\rightarrow\pi_l/v(z)$ into the equations of motion of the exponential representation and attempt to obtain the equations of motion of the linear representation. The substitution into (12) immediately yields

$$\mathrm{e}^{\phi}\partial_z\left(\frac{\mathrm{e}^{-\chi}}{z}\partial_z\varphi\right)+\frac{g_5^2v}{z^3}(\pi_l-v\varphi)=0, \tag{16}$$

which is equivalent to (13) as expected. Showing the equivalence of the other two equations requires a bit more work. First we substitute for π_e in (11) and then simplify the expression,

$$\pi_l'' - \left(\phi' + \frac{3}{z}\right)\pi_l' - \frac{\pi_l}{v}\left(v'' - \phi' v' - \frac{3}{z}v'\right) + m_n^2(\pi_l - v\varphi) = 0. \tag{17}$$

Recalling the equation of motion for $v(z)$ (6), which does not depend on the pseuodscalar representation:

$$v'' - \left(\phi' + \frac{3}{z}\right)v' + \left(\frac{3}{z^2} + \frac{\kappa L^2 v^2}{2z^2}\right)v = 0. \tag{18}$$

Using (18) in (17), we find

$$\pi_l'' - \left(\frac{3}{z} + \phi'\right)\pi_l' + \left(\frac{3}{z^2} + \frac{\kappa L^2 v^2}{2z^2}\right)\pi_l + m_n^2\left(\pi_l - v\varphi\right) = 0, \tag{19}$$

which is equivalent to the other equation of motion of the linear representation (14). The equations of motion are equivalent, confirming that physical results do not depend on the representation.

3.3 Pion Mass Spectrum

We use a modified shooting method to solve the full set of equations of motion in the linear representation. For large-n excitations the numerical technique develops problems with the boundary conditions. As the number of oscillations in the eigenfunctions increase for higher n modes, the routine finds eigenvalues that are skewed to larger values. To uncover the correct asymptotic behavior for large n, we take the large-z limit of (13) and (14). As n increases, the eigenfunction is largely determined by the behavior of the effective potential at large z. At large z, the VEV and dilaton behave as

$$v(z) = (\alpha + \beta)z \equiv \Gamma\frac{z}{L} \tag{20}$$

$$\phi(z) = \lambda z^2. \tag{21}$$

To take the large-z limit of the linear representation, we introduce a new dimensionless parameter, $\xi = \sqrt{\lambda}z$, and expand in ξ. In the linear representation, we find that (**??**) and (**??**) at large ξ become

$$-\pi_k'' + \xi^2\pi_k = \left(\frac{\kappa\Gamma^2}{2\lambda} - 2 + \frac{m_k^2}{\lambda}\right)\pi_k - \frac{m_k^2\Gamma}{\lambda}\varphi_k \tag{22}$$

$$-\varphi_k'' + \xi^2\varphi_k = \frac{g_5^2\Gamma}{\lambda}\left(\pi_k - \Gamma\varphi_k\right) \tag{23}$$

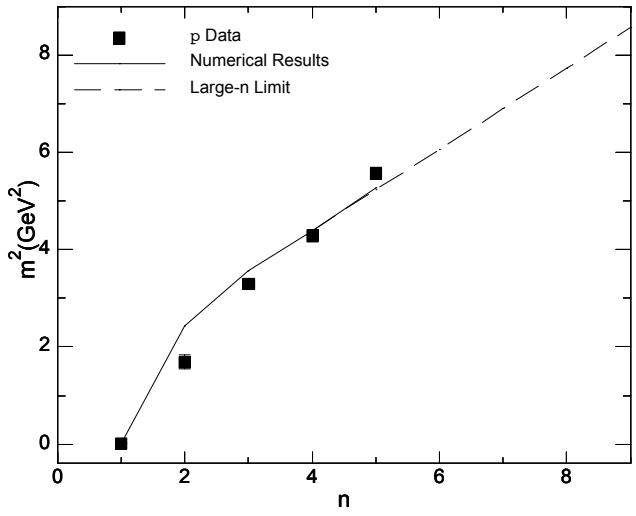

Figure 2: The mass spectrum calculated in the AdS/QCD model is plotted along with the experimental data [13]. The eigenvalues display two characteristics matching the QCD pion spectrum: (1) low-mass ground state and (2) a large gap between the ground state and the first excited state. The large-n approximation clearly follows our calculated eigenvalues for $n \approx 4$.

n	π Data (MeV)	π_l (MeV)	Large-n π_l (MeV)	$\partial_z \pi_e$ (MeV)
1	140	143	-	1440
2	1300 $\pm$ 100	1557	-	1706
3	1816 $\pm$ 14	1887	-	1925
4	2070*	2095	-	2117
5	2360*	2298	2245	2290
6	-	-	2403	2451
7	-	-	2551	2601

Table 2: The observed masses [13] and calculated masses using the linear representations. The large-n limit solutions are valid from $n \approx 4$. The eigenvalues found using the method of [14] are also shown. *Appears only in the further states of [13]

where ($'$) here indicates differentiation with respect to ξ. This set of equations has the form of coupled harmonic oscillators, the equations of motion of which are

$$-\varphi_k'' + \xi^2 \varphi_k = (2k+1)\varphi_k \tag{24}$$
$$-\pi_k'' + \xi^2 \pi_k = (2k+1)\pi_k \qquad k = 0, 1, \ldots . \tag{25}$$

We make the reasonable assumption that $\varphi_k = c_k \pi_k$, which ensures that (22), and (23) have solutions. Using the form of (24) and (25) to solve for m_k^2, and making use of the fact that $\Gamma^2 = \frac{4\lambda}{\kappa}$ ([10]), we find

$$m_k^2 = g_5^2 \Gamma^2 + (2k+1)\lambda. \tag{26}$$

Until now we have not made use of the fact that $z \geq 0$. Because of this, the eigenfunctions φ_n and π_n describe *half* harmonic oscillators with half as many modes; therefore, we must take $k \to 2k$. The mass eigenvalues for large n, where $n = k + 1$, in both representations then become

$$m_n^2 = (4n-3)\lambda + g_5^2 \Gamma^2 \qquad n = 4, 5, \ldots \tag{27}$$

which are also listed in Table 2 and plotted in Figure 2. Combining (27) and the numerical technique, we obtain all the pseudoscalar eigenvalues. On inspection, we find that this method should be trusted over the numerical routine for $n \geq 4$.

3.4 Gell-Mann–Oakes–Renner Relation

In this section we explore the Gell-Mann–Oakes–Renner relation numerically and analytically. Inserting the established equivalence between the exponential and linear representations, $\pi_e = \pi_l / v(z)$, into (17), we obtain

$$\frac{g_5^2 L^2 v^2}{z^2} \partial_z \left(\frac{\pi_l}{v} \right) = m_\pi^2 \partial_z \varphi \,. \tag{28}$$

Following the method of [5], we construct a perturbative solution in m_π where $\varphi(z) = A(0,z) - 1$ and use the established relation

$$f_\pi^2 = - L \frac{\partial_z A(0,z)}{g_5^2 z} \bigg|_{z \to 0.} \tag{29}$$

Integrating (28) yields

$$\frac{\pi(z)}{v(z)} = m_\pi^2 \int_0^z du \, \frac{u^3}{v^2(u)} \frac{\partial_z A(0,u)}{g_5^2 u} \,. \tag{30}$$

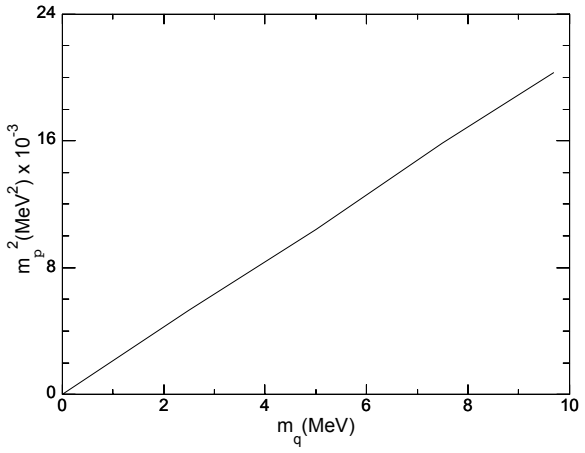

Figure 3: Plot of m_π^2 vs m_q yields a straight line from which the pion decay constant f_π is calculated using (33).

The function $u^3/v^2(u)$ is significant only at small values of $u \sim \sqrt{m_q/\sigma}$, where we may use (29) to relate the derivative on $A(0,u)$ to the pion decay constant, so that

$$\frac{\pi_l}{v} = -\frac{m_\pi^2 f_\pi^2}{2m_q\sigma}\,. \tag{31}$$

We find that letting $\pi_l = -v(z)$ solves the axial-vector field's equation of motion [10]

$$\mathrm{e}^{\phi}\partial_z\left(\frac{\mathrm{e}^{-\phi}}{z}\partial_z A_\mu(q,z)\right) - \frac{q^2}{z}A_\mu(q,z) - \frac{g_5^2L^2v^2}{z^3}A_\mu(q,z) = 0 \tag{32}$$

in the region of small z and as $q \to 0$. As a result, (31) becomes the expected Gell-Mann–Oakes–Renner (GOR) relation,

$$2m_q\sigma = m_\pi^2 f_\pi^2\,. \tag{33}$$

We solve for the ground-state pseudoscalar mass, m_π, for differing values of m_q to ensure that the numerical routine respects the GOR relation and gives a reasonable value for f_π. The results are plotted in Figure 3. The slope of the line in Figure 3 suggests $f_\pi = 90$ MeV, a result consistent with the input parameters as described in [10].

4 The Strange Quark in AdS/QCD

The models in Sections 2 and 3 involve only two quark flavors, describing only the members of the meson octet with no strange quarks. This section adds a third flavor

to the model, allowing for a description of the full meson octet. When the model is expanded to $N_f = 3$, the flavor symmetry must be broken, due to the large value of the strange quark mass. This is accomplished by giving the VEV the following form:

$$X_0 = \frac{1}{2}\begin{pmatrix} v(z) & 0 & 0 \\ 0 & v(z) & 0 \\ 0 & 0 & v_s(z) \end{pmatrix} \tag{34}$$

where $v_s(z)$ is also a solution to (6). This function should also be linear in the IR region, but has different UV boundary conditions corresponding to the strange quark mass and condensate.

The values for these additional parameters can be fixed in one of three ways. Although the Gell-Mann–Oakes–Renner relation is broken for strange quarks, [15] uses this relationship and the mass of the ground state K meson to set these parameters. In [16], there are two methods used to set these constants. The first assumes that the strange quark condensate does not differ from the quark condensate used for the flavor-symmetric theory. The strange quark mass is then set by matching the kaon's ground-state mass in the model to its experimental value. The other method uses a global fit of all the input parameters to a set of fifteen physical observables.

The flavor symmetry breaking comes entirely from the covariant derivative (4). In a flavor-symmetric model, the commutation relations for (4) are trivial: $\{t^a, X_0\} = 2t^a X_0$ and $[t^a, X_0] = 0$. Taking into account the breaking of flavor symmetry yields more involved relations that depend on flavor index. Following [17, 15, 16] , we define z-dependent mass matrices for the vector and axial sectors:

$$\frac{1}{2}M_V^{a\,2}\delta^{ab} = -Tr[t^a, X_0][t^b, X_0] \tag{35}$$

$$\frac{1}{2}M_A^{a\,2}\delta^{ab} = Tr\{t^a, X_0\}\{t^b, X_0\} \tag{36}$$

The $SU(3)$ generators are $t^a = \lambda^a/2$, where λ^a are the Gell-Mann matrices. Working out the commutators yields the following mass matrices

$$M_V^{a\,2} = \begin{cases} 0; & a = 1,2,3 \\ \frac{1}{4}(v_s - v)^2; & a = 4,5,6,7 \\ 0; & a = 8 \end{cases} \tag{37}$$

$$M_A^{a\,2} = \begin{cases} v^2; & a = 1,2,3 \\ \frac{1}{4}(v + v_s)^2; & a = 4,5,6,7 \\ \frac{1}{3}(v^2 + 2v_s^2); & a = 8. \end{cases} \tag{38}$$

The $SU(3)$ index a indicates which members of the meson octet are under consideration: isovectors ($a = 1,2,3$), isodoublets ($a = 4,5,6,7$), and isosinglet $a = 8$.

Expanding the relevant terms and working out the commutation relations, we get the equations of motion in Schrodinger form for the various sectors by following the methods outlined above. The equations of motion for the vector and axial sectors now have the same form, using the appropriate mass matrices:

$$-\Psi_n^{a\prime\prime} + \left(\frac{1}{4}\omega'^2 - \frac{1}{2}\omega'' + \frac{g_5^2 L^2}{z^2} M_\Psi^{a\,2}\right)\Psi_n^a = m_n^2 \Psi_n^a, \tag{39}$$

where $\omega = \phi(z) + \log z$ and $\Psi = V$, A for the appropriate sector. For the isovector particles ($a = 1, 2, 3$), the equations of motion reduce to the forms from [10], as expected. Also, because the vector mass matrix M_V^{a2} is the same for the isovector and isosinglet, their masses will be degenerate in this model. This suggests that the vector isosinglet is the ω meson in the ideal mixing limit [17].

Using the linear representation (9), the equations of motion for the pseudoscalar sector are

$$e^{\phi}\partial_z\left(\frac{e^{-\phi}}{z}\partial_z\varphi_n\right) + \frac{g_5^2 L^2}{z^3}(\xi^a(z)\pi_n - M_A^{a\,2}\varphi_n) = 0 \tag{40}$$

$$z^3 e^{\phi}\partial_z\left(\frac{e^{-\phi}}{z^3}\partial_z\pi_n\right) - \left(\frac{m_X^2}{z^2} - \frac{\kappa L^2(M_A^{a\,2} - M_V^{a\,2})}{2z^2}\right)\pi_n + m_n^2\pi_n = m_n^2\xi^a(z)\varphi_n, \tag{41}$$

where the matrix ξ^a is defined by the relation $2\xi^a(z)\delta_{ab} = \mathrm{Tr}\{t^a, \{t^b, X_0\}\}$. This evaluates to

$$\xi^a(z) = \begin{cases} v; & a = 1, 2, 3 \\ v + v_s; & a = 4, 5, 6, 7 \\ \frac{1}{3}(v + 2v_s); & a = 8. \end{cases} \tag{42}$$

The pseudoscalar equations also reduce to their previous form (13) and (14) when $a = 1, 2, 3$.

5 Conclusion

While AdS/QCD models have enjoyed some phenominological success, a model that fully captures the richness of QCD remains a lofty goal. The work presented above shows the progress that has been made with such models in describing meson phenomenology. The modified soft-wall model has shown good results for the pion sector, and work to include the strange quark is promising. There are several other extensions that can be made to this modified soft-wall model. Baryons, tensor mesons, and glueballs all have yet to be investigated in soft-wall AdS/QCD, leaving much to be uncovered by future research.

References

[1] J. M. Maldacena, Advances in Theoretical Mathematical Physics **2**, 231+ (1998), hep-th/9711200.

[2] I. R. Klebanov and E. Witten, Nuclear Physics B **556**, 89+ (1999), hep-th/9905104.

[3] F. Jugeau, (2009), 0902.3864.

[4] H. J. Kwee and R. F. Lebed, Physical Review D **77** (2008), 0712.1811.

[5] J. Erlich, E. Katz, D. T. Son, and M. A. Stephanov, Physical Review Letters **95** (2005), hep-ph/0501128.

[6] J. Polchinski and M. J. Strassler, Physical Review Letters **88**, 031601+ (2002).

[7] M. Shifman, (2005), hep-ph/0507246.

[8] A. Karch, E. Katz, D. T. Son, and M. A. Stephanov, Physical Review D **74** (2006), hep-ph/0602229.

[9] M. Shifman and A. Vainshtein, Physical Review D **77**, 034002+ (2008).

[10] T. Gherghetta, J. I. Kapusta, and T. M. Kelley, Physical Review D **79**, 076003+ (2009).

[11] T. M. Kelley, S. P. Bartz, and J. I. Kapusta, Physical Review D **83** (2011), 1009.3009.

[12] P. Colangelo, F. De Fazio, F. Giannuzzi, F. Jugeau, and S. Nicotri, Physical Review D **78** (2008), 0807.1054.

[13] K. Nakamura, Journal of Physics G: Nuclear and Particle Physics **37**, 075021+ (2010).

[14] Y.-Q. Sui, Y.-L. Wu, Z.-F. Xie, and Y.-B. Yang, Physical Review D **81** (2010), 0909.3887.

[15] Y.-Q. Sui, Y.-L. Wu, and Y.-B. Yang, (2010), 1012.3518.

[16] Z. Abidin and C. E. Carlson, Physical Review D **80** (2009), 0908.2452.

[17] J. P. Shock and F. Wu, Journal of High Energy Physics **2006**, 023+ (2006).